THE JOURNAL OF BIOLOGICAL CHEMISTRY VOL. 289, NO. 40, pp. 27562–27570, October 3, 2014

Tyrosine-based Signal Mediates LRP6 Receptor Endocytosis and Desensitization of Wnt/β-Catenin Pathway Signaling*

Received for publication, April 1, 2014, and in revised form, August 18, 2014 Published, JBC Papers in Press, August 20, 2014, DOI 10.1074/jbc.M113.533927

Chia-Chen Liu[‡§], **Takahisa Kanekiyo**[§], **Barbara Roth**[§], **and Guojun Bu**[‡§1]

From the [‡]*Fujian Provincial Key Laboratory of Neurodegenerative Disease and Aging Research, Institute of Neuroscience, College of Medicine, Xiamen University, Xiamen, Fujian 361005, China and the* [§]*Department of Neuroscience, Mayo Clinic, Jacksonville, Florida 32224*

Background: LRP6 is an essential co-receptor for Wnt/β-catenin signaling, which controls various biological pathways.
Results: LRP6 tyrosine mutant exhibited longer half-life and increased lipid raft distribution, phosphorylation, and signaling.
Conclusion: Clathrin-mediated endocytosis of LRP6 mediates its degradation, whereas caveolae-dependent pathway promotes Wnt/β-catenin signaling.
Significance: Understanding the molecular mechanisms underlying LRP6 endocytosis and Wnt/β-catenin signaling will help the development of therapeutic methods targeting this pathway.

Wnt/β-catenin signaling orchestrates a number of critical events including cell growth, differentiation, and cell survival during development. Misregulation of this pathway leads to various human diseases, specifically cancers. Endocytosis and phosphorylation of the LDL receptor-related protein 6 (LRP6), an essential co-receptor for Wnt/β-catenin signaling, play a vital role in mediating Wnt/β-catenin signal transduction. However, its regulatory mechanism is not fully understood. In this study, we define the mechanisms by which LRP6 endocytic trafficking regulates Wnt/β-catenin signaling activation. We show that LRP6 mutant with defective tyrosine-based signal in its cytoplasmic tail has an increased cell surface distribution and decreased endocytosis rate. These changes in LRP6 endocytosis coincide with an increased distribution to caveolae, increased phosphorylation, and enhanced Wnt/β-catenin signaling. We further demonstrate that treatment of Wnt3a ligands or blocking the clathrin-mediated endocytosis of LRP6 leads to a redistribution of wild-type receptor to lipid rafts. The LRP6 tyrosine mutant also exhibited an increase in signaling activation in response to Wnt3a stimulation when compared with wild-type LRP6, and this activation is suppressed when caveolae-mediated endocytosis is blocked. Our results reveal molecular mechanisms by which LRP6 endocytosis routes regulate its phosphorylation and the strength of Wnt/β-catenin signaling, and have implications on how this pathway can be modulated in human diseases.

The Wnt/β-catenin signaling pathway regulates various events during embryonic development, including cell proliferation, survival, migration and polarity, specification of cell fate, and self-renewal (1–3). As such, abnormal Wnt/β-catenin signaling leads to defects in embryonic development as well as a variety of human diseases, such as cancer (4) and Alzheimer disease (5). The Wnt family consists of 19 secreted glycoproteins (6) that engage two cell surface receptors: the Frizzled (Fz)[2] family (7) and low density lipoprotein receptor (LDLR)-related protein 5/6 (LRP5/6) (8). Wnt stimulation induces the phosphorylation of LRP5/6, which leads to a suppression of glycogen synthase kinase 3β (GSK3β)-mediated β-catenin phosphorylation (9, 10). Consequently, β-catenin accumulates and translocates to the nucleus, where it activates target gene expression (1, 11).

Endocytosis of cell surface receptors is an important regulatory event in signal transduction including Wnt/β-catenin signaling (12, 13). Studies show that the clathrin-mediated pathway plays a crucial role in terminating cell signaling by down-regulating transmembrane signaling receptors (14, 15). In some cases when signaling is constitutively active, however, receptors may undergo continuous rounds of endocytosis and recycling, thus protecting the receptors from degradation (16–18). Clathrin-independent internalization occurs mostly at lipid rafts, which are membrane microdomains that consist of a dynamic assembly of cholesterol and glycosphingolipids (19). Caveolin mediates some of the clathrin-independent events, forming membrane invaginations (caveolae) on lipid rafts (20). This pathway has been shown to function as a platform for receptor-mediated signaling by facilitating the sequestration of receptors and signaling molecules within caveolae (21, 22). Cell surface receptors that traffic between the plasma membrane and endocytic compartments contain signals within their cytoplasmic tails that enable their efficient recruitment into endocytic vesicles. Several classes of endocytosis signals have been identified that target surface proteins to clathrin-coated vesicles (23). Tyrosine-based motifs NP*X*Y or Y*XX*Ø (where *X* can be any amino acid and Ø is an amino acid with a bulky hydrophobic group) within the cytoplasmic tail were initially identified in the low density lipoprotein receptor and transferrin receptor (24).

* This work was supported, in whole or in part, by National Institutes of Health Grants R01 AG035355 and P01 AG030128 (to G. B.) and Alex's Lemonade Stand Foundation Young Investigator Award (to T. K.).
[1] To whom correspondence should be addressed: Dept. of Neuroscience, Mayo Clinic, 4500 San Pablo Rd., Jacksonville, FL 32224. Tel.: 904-956-3419; Fax: 904-953-7370; E-mail: bu.guojun@mayo.edu.

[2] The abbreviations used are: Fz, Frizzled; Mesd, mesoderm development; Nys, nystatin; MDC, monodansylcadaverine; Dkk1, Dickkopf1; Krm, Kreman; Cav-1, caveolin-1; CM, conditioned medium; TCF, transfection grade T cell factor.

In addition, ligand-induced phosphorylation of serine residues can also serve as a signal for receptor endocytosis, noticeably for members of the G protein-coupled receptor family (25).

LRP6 contains multiple potential endocytosis motifs within its cytoplasmic region, including two tyrosine-based signals and five conserved PPP(S/T)P motifs, whose phosphorylation is necessary for Wnt/β-catenin signaling (10). Therefore, we hypothesize that specific sequence motifs in the intracellular domain of LRP6 regulate its endocytosis and signal transduction. Here we defined the mechanisms underlying LRP6 endocytosis, phosphorylation, and Wnt/β-catenin signaling using unique LRP6 mutants.

EXPERIMENTAL PROCEDURES

Cloning of LRP6 Wild-type and Mutants—LRP6 mutations were generated by site-directed mutagenesis using the QuikChange mutagenesis kit (Stratagene), according to the manufacturer's instructions. All constructs were verified by sequencing. LRP6 WT and mutants, each of which contains an HA tag at its N terminus, were then subcloned into Flp-In expression vectors (Invitrogen). Upon recombinase-mediated DNA recombination, LRP6 was integrated into the genome at a specific location.

Cell Culture and Reagent—Flp-In HEK293 cells (Invitrogen) were maintained in DMEM containing glucose (4.5 g/liter), L-glutamine, 1% penicillin/streptomycin and supplemented with 10% FBS. For stable clone generation, the WT and LRP6 mutants in the pcDNA5/FRT expression vector were transfected into Flp-In HEK293 cells using the FuGENE 6 transfection reagent (Roche Applied Science). After 48 h, cells were split into a 15-cm^2 dish. After cells attached to the dish, fresh medium with hygromycin B (100 μg/ml) was used to select resistant cells in which the cDNA construct had been integrated into the Flp-In site. The cells were fed with selection medium every 5 days until colonies could be identified. 10–15 individual stable clones for LRP6 WT and each mutant were picked and amplified for further characterization. Pitstop 2 was obtained from Abcam. Human Cav-1 siRNA was purchased from Dharmacon. To isolate lipid raft-associated proteins, FOCUS Global Fractionation kit (G-Biosciences) was used according to the manufacturer's instructions.

Flow Cytometry—Cells were detached by nonenzymatic cell dissociation solution (Sigma). For total LRP6 analysis, cells were treated with 0.1% saponin in PBS for 30 min prior to incubation with antibody. For cell surface LRP6, cells were incubated with primary antibody without permeabilization. Successive incubations with anti-HA IgG (30 μg/ml) for HA-LRP6 and anti-mouse Alexa Fluor 488 (Molecular Probes) were carried out at 4 °C for 1 h. As a control, background fluorescence intensity was assessed in the absence of the primary antibody. All measurements were performed on a FACSCalibur (BD Biosciences). Histograms were generated using the CellQuest software, and the mean values, after subtraction of controls, were compared among samples.

Determination of LRP6 Half-life—Cells were incubated with cycloheximide (100 μg/ml, Sigma) to inhibit protein synthesis. Following incubation for 0, 0.5, 1, 2, 4, or 8 h, cells were lysed and subjected to Western blot.

Antibody Uptake and Immunofluorescent Staining—Anti-HA IgG was labeled using the Alexa Fluor 488 protein labeling kit (Molecular Probes). Cells were cultured on the poly-D-lysine-coated glass bottom culture dishes (MatTek Corp.) at 37 °C for at least 24 h before experiments. Cells were incubated with Alexa Fluor 488-labeled anti-HA IgG for 1 h at 4 °C and shifted to 37 °C for 0, 15, 30, 60, and 120 min to induce LRP6 internalization. After incubation at 37 °C, cells were fixed with 4% paraformaldehyde for 20 min. For immunofluorescence staining, cells were washed with PBS and fixed with 4% paraformaldehyde in PBS for 20 min at room temperature. Cells were then blocked with blocking buffer (PBS containing 0.5% BSA) and permeabilized with PBS containing 0.2% Triton X-100. Afterward, the cells were incubated with primary LRP6 or EEA1 antibodies for 2 h at room temperature followed by an Alexa Fluor-conjugated secondary antibody for 1 h (Molecular Probes). The cell surface LRP6 was stained without permeabilization. Stained cells were viewed by confocal laser-scanning fluorescence microscopy (model LSM 510 inverted; Carl Zeiss). To quantify the levels of cell surface LRP6, 10–12 fields per WT or mutant samples were chosen, and the fluorescent intensity was measured by ImageJ.

Kinetic Analysis of Endocytosis—Kinetic analysis of receptor-mediated endocytosis was carried out as described previously (26). Briefly, cells were cultured in poly-D-lysine-coated 12-well plates 24 h before experiments. Cells were rinsed twice with cold PBS and then incubated in 0.5 ml of ice-cold ligand binding buffer (DMEM containing 0.6% bovine serum albumin) containing 1 nM ^{125}I-Mesd for 1 h. After binding, prewarmed binding buffer was added to the cells, and the plates were placed in a 37 °C water bath for 0, 5, 10, 20, 30, and 60 min to initiate internalization. The plates were then placed on ice, and the ligand binding buffer was replaced with ice-cold stop/strip solution (PBS, pH 2.0). Ligands that remained on the cell surface were stripped twice by incubating cell monolayers with ice-cold stop/strip solution for a total of 10 min and counted. Cell monolayers were then solubilized with low SDS lysis buffer (6.25 mM Tris, pH 6.8, 0.2% SDS, 10% glycerol, and bromphenol blue) to release internalized radioactivity. The sum of internalized ligands plus those on the surface after each assay was used as the maximum potential internalization. The fraction of internalized ligand at each time point was calculated and plotted.

Co-immunoprecipitation—Cells were lysed, and the lysates were precleared for at least 2 h with protein-A-agarose beads and then incubated with an antibody overnight at 4 °C. The immunocomplexes were precipitated with protein-A-agarose beads for 1 h, washed three times with PBS, and boiled in SDS sample buffer containing β-mercaptoethanol. The supernatants were subjected to SDS-PAGE and Western blotting.

Immunoblotting—Cells were lysed in PBS containing 1% Triton, protease inhibitor cocktail (Roche Applied Science), and 1 mM PMSF at 4 °C for 30 min. Equal quantities of protein were subjected to 7.5, 12.5, or 4–15% SDS-PAGE and transferred to Immobilon-P membrane (Millipore). Membranes were blocked in PBS 5% nonfat dried milk with 0.05% Tween 20 and subjected to incubation with primary and secondary antibodies. Membrane probed with horseradish peroxidase-conjugated

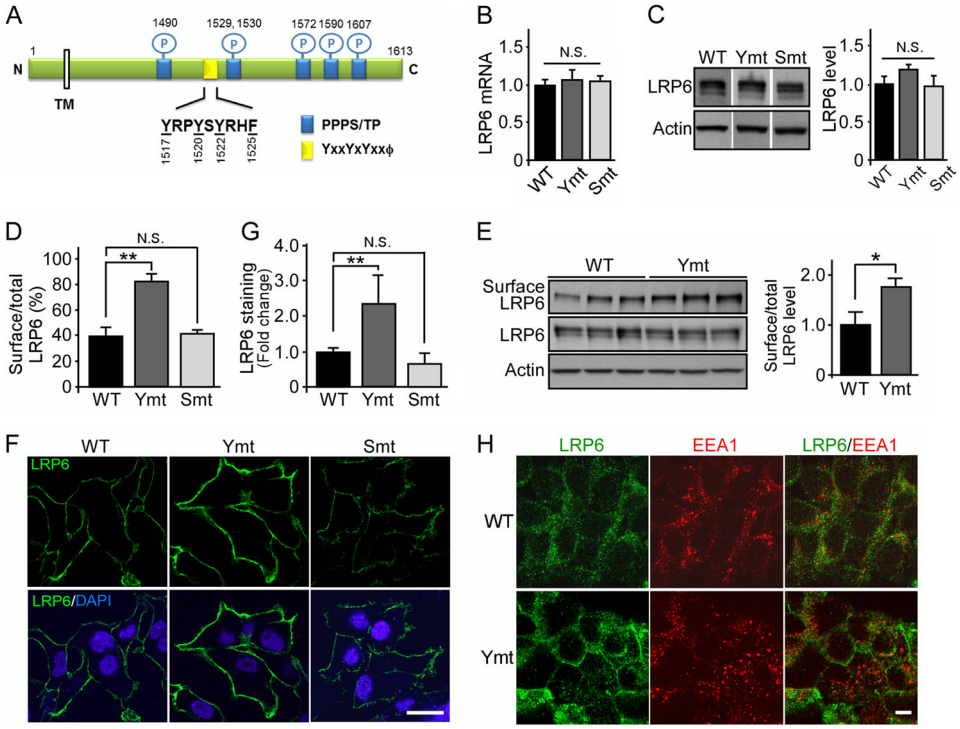

FIGURE 1. **LRP6 tyrosine mutant displays increased cell surface distribution.** *A*, a schematic diagram of potential endocytosis motifs in the LRP6 cytoplasmic tail. The LRP6 tail contains tyrosine-based motifs (*yellow*) and five highly conserved PPP(S/T)P motifs in which the Ser/Thr residues can be phosphorylated (*blue*). *TM*, transmembrane; *P*, phosphorylation; *N*, N terminus; *C*, C terminus. *B*, LRP6 mRNA expression in HEK293 cells stably expressing LRP6 WT or mutants was analyzed by real-time PCR. *Ymt*, tyrosine mutant; *Smt*, serine/threonine mutant. *C*, LRP6 expression in these cells was analyzed by Western blot and quantified. *D*, cells stably expressing LRP6 WT or mutants were labeled with anti-HA antibody, and the levels of cell surface and total cellular LRP6 were assessed by flow cytometry. *E*, the cell surface levels of LRP6 were quantified by cell surface biotinylation assay. Cell surface proteins from cells stably expressing LRP6 WT or tyrosine mutant were biotinylated, isolated with avidin-conjugated beads, and immunoblotted with HA antibody against LRP6. Cell surface and total LRP6 in cell lysates was measured by Western blot. *F* and *G*, cells stably expressing LRP6 WT or mutants were fixed without permeabilization and stained for LRP6 with anti-HA (*green*), and the nucleus was stained with DAPI (*blue*) (*F*). *Scale bars*, 5 μm. Fluorescence measurements for LRP6 were performed with ImageJ (*G*). *H*, cells stably expressing LRP6 WT or tyrosine mutant were fixed, permeabilized, and stained for LRP6 with anti-HA (*green*) and co-stained with anti-EEA1 (*red*). Representative confocal laser scanning microscopy images were shown. *Scale bars*, 5 μm. Data are representative of three independent experiments. Data represent mean ± S.D. *N.S.*, not significant; *, $p < 0.05$. **, $p < 0.01$.

secondary antibody (Amersham Biosciences) was visualized by ECL detection system (Pierce) and exposed to film. The gel image was scanned by the ChemiDoc imaging system (Bio-Rad) and quantified. In some experiments, membrane was probed with LI-COR IRDye secondary antibodies and detected using the Odyssey infrared imaging system (LI-COR). The following antibodies were used in this study: LRP6, phospho-LRP6 (Ser-1490) (Cell Signaling); β-catenin antibody (BD Pharmingen); transferrin receptor (Invitrogen); caveolin-1 (Santa Cruz Biotechnology); actin and clathrin antibodies (Sigma).

Fractionation of Plasma Membrane—Cells expressing WT and mutant LRP6 were lysed in 0.25 ml of ice-cold TNE buffer (25 mM Tris-HCl; pH 7.4, 150 mM NaCl, and 5 mM EDTA) containing 0.4% Triton X-100, 1 mM PMSF, protease inhibitor cocktail, and phosphatase inhibitors. Cells were then homogenized with a Dounce homogenizer (40 strokes) and passaged through a 25-gauge needle. Each lysate (0.25 ml) was mixed with 0.25 ml of 80% (w/v) sucrose in TNE and overlaid with 1 ml of 35% sucrose in TNE followed by 0.5 ml of 5% sucrose in TNE. The gradients were centrifuged at 54,000 rpm for 16 h at 4 °C in a TLS55 rotor (Beckman). 120-μl fractions were harvested from the top of the gradient. Aliquots were subjected to SDS-PAGE and probed with the indicated antibodies.

Quantitative Real-time PCR—Total RNAs isolated from Flp-In HEK293 cells expressing WT or mutant LRP6 using TRIzol (Invitrogen) and the RNeasy mini kit (Qiagen) were reverse-transcribed with the Superscript first-strand synthesis system (Invitrogen). The reaction mix was subjected to quantitative real-time PCR to detect expression levels of LRP6. All primers for real-time PCR were ordered from SABiosciences. Triplicate reactions were prepared using a 25-μl mixture containing Platinum SYBR Green quantitative PCR SuperMix UDG (Invitrogen). Real-time quantification was performed on a Bio-Rad iCycler iQ system. All data were normalized to the endogenous actin expression.

GST-E-cadherin Pulldown Assay—The assay was carried out as described previously (27). Cells were lysed for 30 min at 4 °C. Protein concentrations in lysates were quantified, and equal quantities of total proteins from different samples were incubated with GST-E-cadherin-Sepharose beads for 4 h at 4 °C. After incubation, the beads were washed three times, and the bound proteins were eluted and separated via SDS-PAGE. Western blotting was performed using antibody to β-catenin.

Luciferase Reporter Assay—Cells were transfected with TOP-Flash or FOPFlash plasmids (Millipore) and treated with conditioned medium from parental L cell or Wnt3a-expressing cultures for 24 h. A β-gal reporter cDNA was co-transfected to normalize data for transfection efficiency. The luciferase and β-gal activities were measured by the luciferase and β-gal assay

systems, respectively, following the manufacturer's instructions (Promega).

Statistical Analysis—All quantified data represent an average of triplicate samples. Error bars represent S.D. Statistical analyses were performed using Student's *t* test when one group was compared with the control group. When more than two groups were compared, analysis of variance with Bonferroni's multiple comparison post hoc test was used to determine the significance. $p < 0.05$ was considered significant.

RESULTS

Tyrosine-based Motifs within the LRP6 Cytoplasmic Tail Serve as an Endocytosis Signal—Receptor-mediated endocytosis is driven by signals within the intracellular domains of cell surface receptors. The LRP6 cytoplasmic tail contains two such tyrosine-based signals: Y*XXY* and Y*XX*F motifs (Fig. 1*A*). To examine their roles in LRP6 endocytosis, we mutated both motifs from YRPYSYRHF to ARPASARHA (hereafter referred to as tyrosine mutant). In addition, given that Wnt stimulates LRP6 phosphorylation on the PPP(S/T)P motif, which is critical for axin binding and its signaling activity (10), we sought to examine whether LRP6 phosphorylation plays a role in regulating its endocytosis. As such, we mutated the critical Ser/Thr residues within all five PPP(S/T)P signaling motifs to Ala (hereafter referred to as serine/threonine mutant) (Fig. 1*A*).

Because variation in transfection efficiency among different LRP6 mutant constructs and heterogeneous expression within a given cell population might result in experimental variability, we used the Flp-In system to establish stable HEK293 cell lines in which a single copy of wild-type LRP6 (hereafter referred to as WT) or either of the mutants was introduced into a defined chromatin location. Using real-time PCR (Fig. 1*B*) and Western blot analysis (Fig. 1*C*), HEK293 stable clones exhibiting similar levels of WT or mutant LRP6 were selected for the study.

To investigate the role of specific motifs in LRP6 endocytosis, we first examined the cell surface distribution of WT and mutant LRP6 by FACS analysis. In cells expressing the LRP6 tyrosine mutant, the amount of cell surface LRP6 was significantly increased when compared with cells expressing LRP6 WT; however, in cells expressing the serine/threonine mutant, there was no increase in LRP6 cell surface levels (Fig. 1*D*). To further confirm this result, we performed a cell surface biotinylation analysis to quantify the cell surface level of LRP6. Cell surface proteins were labeled with sulfo-NHS-LC-biotin, isolated with streptavidin beads, and probed with anti-LRP6 antibody. Consistent with results from FACS analysis, we found that the cell surface level of LRP6 was significantly increased in cells expressing the LRP6 tyrosine mutant (Fig. 1*E*). The immunofluorescence staining of LRP6 also revealed that the tyrosine mutant exhibited an increased cell surface staining of LRP6 when compared with WT under nonpermeabilized condition (Fig. 1, *F* and *G*). Under permeabilized conditions, LRP6 WT was mostly distributed in the endosomal compartments and partially co-localized with EEA1, a marker for early endosome. Importantly, a significant increase in the cell surface distribution of LRP6 tyrosine mutant when compared with LRP6 WT was observed with little co-localization with EEA1 (Fig. 1*H*). Together, these results suggest that disruption of tyrosine-based motifs of LRP6, but not the phosphorylation motifs, impairs its internalization and results in an increase in its cell surface distribution.

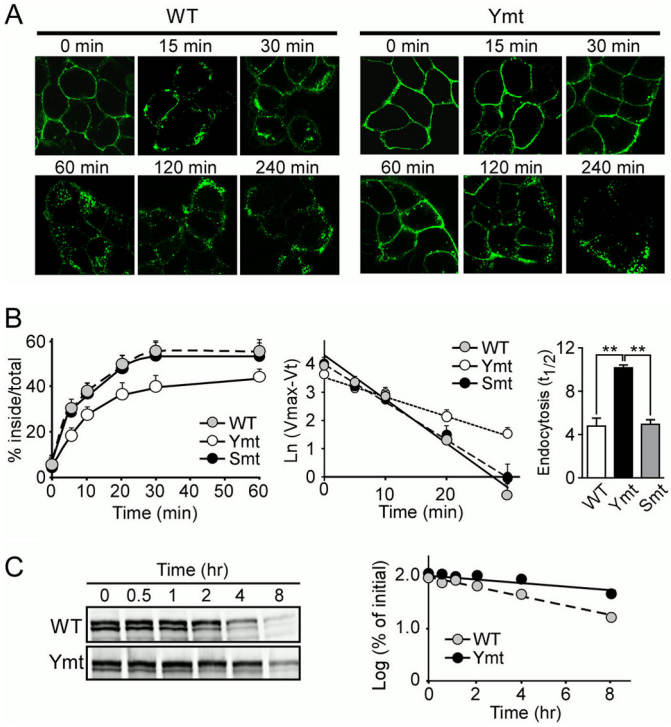

FIGURE 2. **Mutation of tyrosine-based motifs in the LRP6 cytoplasmic tail impairs its endocytosis.** *A*, HEK293 cells stably expressing the LRP6 WT or tyrosine mutant (*Ymt*) were incubated with Alexa Fluor 488-labeled anti-HA IgG for 1 h at 4 °C and then shifted to 37 °C for increasing periods of time to initiate endocytosis. Fluorescence images were obtained by confocal microscopy. *Scale bars*, 5 μm. *B*, cells stably expressing LRP6 WT, tyrosine (*Ymt*), and serine/threonine mutants (*Smt*) were subjected to a kinetic analysis of endocytosis using ^{125}I-labeled Mesd (5 nM). The sum of ligand that was internalized, and that which remained on the cell surface at the end of the assay was used as the maximum potential internalization. The fraction of internalized ligand after each time point was calculated and plotted (*left panel*). Data represent mean ± S.D. Then, *Ln* (V_{max} (maximum internalization) − V^t (internalization % at each time point)) was calculated and plotted against each time point (*middle panel*). The half-time ($t_{1/2}$) for the internalization of LRP6 was then calculated as $t_{1/2} = ln2/k = 0.693/(\text{slope})$ and is shown as a bar graph (*right panel*). Data represent mean ± S.D. **, $p < 0.01$. *C*, cells stably expressing LRP6 WT or tyrosine mutant were treated with cycloheximide and lysed at 0, 0.5, 1, 2, 4, and 8 h following the treatment. Lysates were then immunoblotted for LRP6. The half-life of LRP6 was calculated on the basis of the slope of the semilog plot of percentage of change in LRP6 *versus* time.

To further study whether tyrosine-based motifs of LRP6 serve as an endocytotic signal, we next monitored LRP6 endocytosis by pulse-chase analysis. Cells expressing HA-tagged LRP6 WT or tyrosine mutant were first incubated with fluorescent-labeled HA antibody at 4 °C, which labels LRP6 at the plasma membrane (Fig. 2*A*). Upon warming up to 37 °C, a substantial amount of LRP6 was internalized in cells expressing LRP6 WT with significant endocytosis seen after 15–30 min. On the other hand, LRP6 was retained mostly at the cell surface even after 60 min of incubation in cells expressing tyrosine mutant (Fig. 2*A*).

To directly measure endocytosis rates of LRP6 WT and mutants, ^{125}I-labeled Mesd, a specialized chaperone and a ligand for LRP6 (28, 29), was utilized to perform the endocytosis assay. The fraction of internalized ligand after each time point was calculated and plotted (Fig. 2*B*). The half-times ($t_{1/2}$) for the

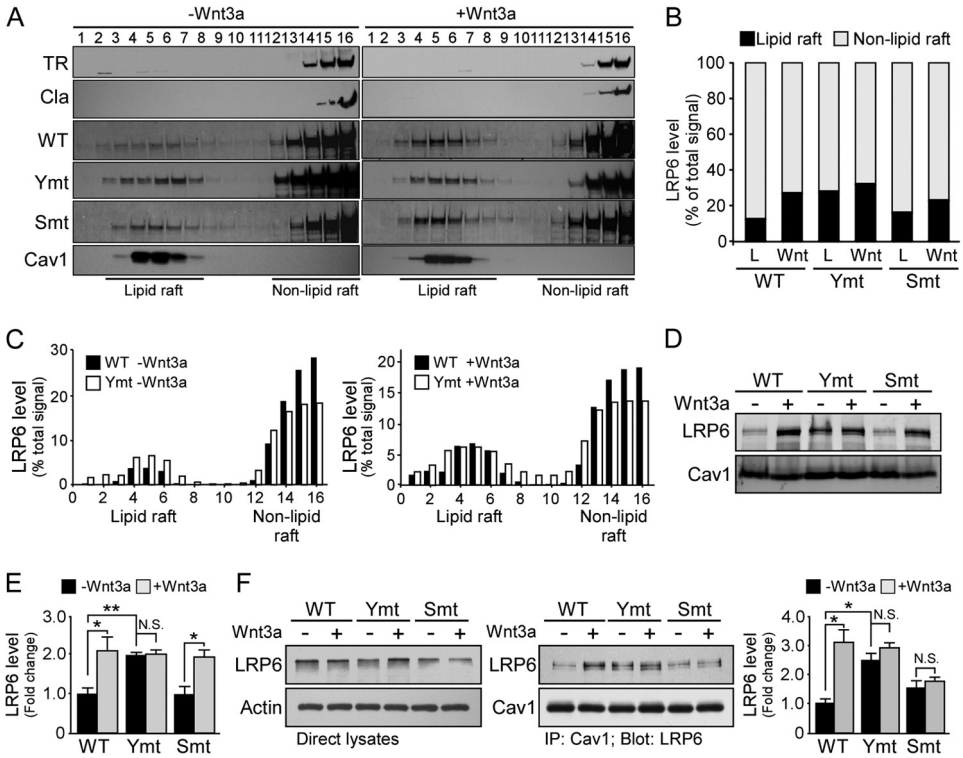

FIGURE 3. **Distribution of LRP6 with defective tyrosine-based motifs in lipid rafts.** *A*, lysates of cells expressing WT and LRP6 mutants treated with control conditioned medium (CM) or Wnt3a CM were fractionated by sucrose density gradient centrifugation and probed with anti-LRP6 antibody. Endogenous Cav-1 and clathrin (*Cla*), which indicate the respective positions of lipid rafts and non-lipid raft factions, respectively, were detected using specific antibodies. *TR*, transferrin receptor; *Ymt*, tyrosine mutant; *Smt*, serine/threonine mutant. *B*, densitometric quantification of Western blot signals from *A*. The LRP6 intensities in all fractions were added up as total signals. The percentage of LRP6 levels in the lipid raft enriched fractions (fractions 2–8) and non-lipid raft fractions was calculated and is shown. *C*, the LRP6 levels in each fraction are plotted as *% total signal*. *D*, cells expressing WT and LRP6 mutants were treated with control CM or Wnt3a CM for 16 h. The membrane proteins concentrated in caveolin-rich membranes and lipid rafts were isolated and subjected to Western blot analysis. *E*, densitometric quantification of Western blot signals from *D*. *N.S.*, not significant; *, $p < 0.05$; **, $p < 0.01$. *F*, co-immunoprecipitation of LRP6 and caveolin-1. Lysates of cells expressing WT and LRP6 mutants were immunoprecipitated with anti-Cav-1, and the immunoprecipitates were probed with anti-LRP6 antibody. Data represent mean ± S.D. *, $p < 0.05$.

internalization of LRP6 WT and the serine/threonine mutant were determined to be 4.85 ± 0.73 and 5.02 ± 0.42 min, respectively, whereas LRP6 tyrosine mutant exhibited a much slower endocytosis rate with a $t_{1/2}$ of 10.22 ± 0.27 min (Fig. 2*B*). These results further indicate that tyrosine-based motifs might serve as an endocytotic signal within the LRP6 cytoplasmic tail. In addition, we found that the LRP6 tyrosine mutant exhibited a longer half-life when compared with that of LRP6 WT when cycloheximide was used to block protein synthesis (Fig. 2*C*). The $t_{1/2}$ for LRP6 WT was 3.68 h, and the $t_{1/2}$ for tyrosine mutant was 7.07 h, indicating that impairment of LRP6 internalization prolonged its half-life.

Redistribution of LRP6 Endocytosis Mutant to Caveolae Enhances Its Phosphorylation and Wnt/β-Catenin Signaling—To determine whether inhibition of endocytosis or phosphorylation of LRP6 alters its internalization route in the presence or absence of Wnt3a stimulation, lysates of cells expressing LRP6 WT or mutants were subjected to fractionation by sucrose gradient. Of note, the LRP6 tyrosine mutant showed increased distribution of LRP6 in lipid rafts when compared with LRP6 WT (Fig. 3, *A*–*C*). These results suggest that inhibition of LRP6 internalization through the clathrin-mediated pathway redistributes LRP6 to raft fractions. In addition, Wnt3a administration also increased LRP6 distribution in the lipid raft fractions (Fig. 3, *A* and *B*). To further validate this observation, we isolated lipid raft-associated membrane proteins from cells expressing LRP6 WT or mutants. Consistent with our previous findings, we found that mutation of tyrosine-based motifs enhanced LRP6 distribution in lipid rafts in the absence of Wnt3a stimulation (Fig. 3, *D* and *E*). To investigate whether disruption of LRP6 phosphorylation or internalization affects its association with caveolin, we examined their interactions in the presence or absence of Wnt3a ligand by co-immunoprecipitation analysis. Although Wnt3a stimulation significantly increased the association of LRP6 WT with caveolin (Fig. 3*F*), the LRP6 tyrosine mutant exhibited a stronger association with caveolin when compared with WT even in the absence of Wnt stimulation (Fig. 3*F*). These results indicate that tyrosine-based signals play an important role in determining LRP6 internalization routes as well as serve as an endocytosis motif.

A crucial step in Wnt/β-catenin signaling activation is the phosphorylation of PPP(S/T)P motifs in the intracellular domain of LRP6 via casein kinase 1γ (CK1γ) and GSK3β. The phosphorylation of LRP6 stabilizes the Wnt/β-catenin signaling transducer β-catenin, resulting in signaling activation (10). To investigate whether disruption of clathrin-mediated endocytosis of LRP6 affects its phosphorylation and Wnt/β-catenin signaling activation, we assessed the phosphorylation status of LRP6 WT and mutants by Western blot analysis and the strength of Wnt/β-catenin signaling by TCF reporter assay. As

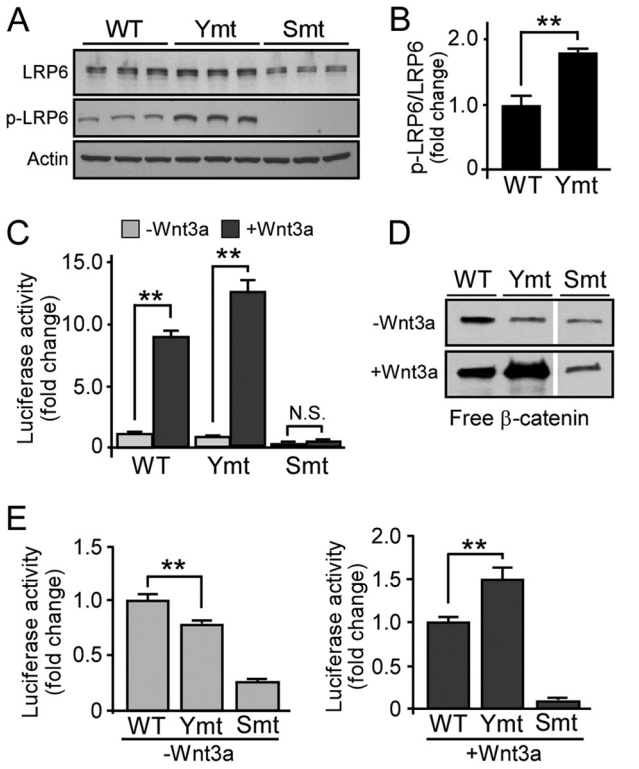

FIGURE 4. **Enhanced phosphorylation and Wnt/β-catenin signaling activation of LRP6 with defective tyrosine-based motifs.** *A*, lysates of cells expressing WT or LRP6 mutants were subjected to Western blot analysis and probed with anti-LRP6 or anti-phospho-LRP6 (*p-LRP6*) (Ser-1490) antibodies. *Ymt*, tyrosine mutant; *Smt*, serine/threonine mutant. *B*, the ratios of phospho-LRP6 *versus* total LRP6 (*p-LRP6/LRP6*)were compared between WT and tyrosine mutant. *C–E*, cells expressing WT or mutant LRP6 were transfected with TOPFlash/FOPFlash plasmids and were subsequently incubated with control CM or Wnt3a CM for 16 h. Wnt/β-catenin signaling activity was evaluated with TOPFlash TCF-luciferase reporter (*C* and *E*) or GST-E-cadherin pulldown assays (*D*). To clearly illustrate the signal activation in the presence or absence of Wnt3a stimulation, the activities were plotted together (*C*) or separately (*E*). Data are representative of three independent experiments. Data represent mean ± S.D. *N.S.*, not significant; **, $p < 0.01$.

expected, Wnt3a significantly induced Wnt/β-catenin signaling activation in both LRP6 WT and tyrosine mutant, whereas the serine/threonine mutant was not phosphorylated and exhibited minimal signaling activation (Fig. 4, *A–C*). Interestingly, LRP6 tyrosine mutant is phosphorylated to a greater degree in the absence of Wnt3a treatment (Fig. 4*A*), whereas displaying a reduced basal level of Wnt signaling when compared with WT (Fig. 4, *D* and *E*). In addition, Wnt3a stimulation induced a greater activation of Wnt/β-catenin in cells expressing LRP6 tyrosine mutant when compared with WT (Fig. 4, *D* and *E*). Taken together, these results suggest that lipid raft distribution of LRP6 led to an increase in its phosphorylation; however, it is not sufficient to induce Wnt/β-catenin signaling activation in the absence of Wnt ligands.

Blocking of Caveolae-mediated, but Not Clathrin-mediated Endocytosis Reduces LRP6 Phosphorylation and Wnt/β-Catenin Signaling—To examine whether alteration of LRP6 internalization routes affects its phosphorylation and signal transduction, cells expressing WT or LRP6 mutants were treated with nystatin (Nys) or monodansylcadaverine (MDC), inhibitors for caveolae or clathrin-mediated endocytosis, respectively. We found that Nys significantly inhibited LRP6 phosphorylation both in the presence and in the absence of Wnt3a stimulation, whereas inhibition of clathrin-mediated endocytosis via MDC had no significant effect (Fig. 5*A*). We also examined which internalization route is important for Wnt3a signaling activation. Blocking caveolin-mediated endocytosis by Nys suppressed Wnt signaling (Fig. 5*B*). Furthermore, cells expressing LRP6 tyrosine mutant exhibit higher Wnt signaling activation, which is suppressed by Nys treatment (Fig. 5*B*). As phosphorylation of LRP6 is required for signaling activation, we tested whether knockdown of caveolin-1 by siRNA affects LRP6 phosphorylation (Fig. 5*C*). Consistent with the effects via Nys treatment, knockdown of caveolin-1 suppressed LRP6 phosphorylation (Fig. 5, *D* and *E*). Interestingly, inhibition of clathrin-mediated endocytosis via MDC, or Pitstop 2, a more selective clathrin inhibitor, slightly increased basal level of signaling in the absence of Wnt3a treatment (Fig. 5, *F* and *G*), whereas MDC has no significant effect in the presence of Wnt3a (Fig. 5*F*). Together, these results indicate that caveolin-mediated endocytosis of LRP6 is critical for Wnt3a-induced signaling activation.

DISCUSSION

The Wnt/β-catenin signaling pathway controls a myriad of biological phenomena throughout development and in adulthood. Aberrant activation of this pathway underlies the pathogenesis of several human diseases (30). Thus, it is critical to understand how Wnt/β-catenin signaling is regulated under physiological conditions to develop better therapeutic methods against diseases resulting from misregulation of this pathway.

Given the critical role of Wnt signaling cascade, intricate control systems have evolved to regulate its function. Wnt/β-catenin signaling is tightly modulated by secreted ligands or antagonists that bind to LRP6 at the cell surface (11). In addition to the Wnt ligands, Dickkopf1 (Dkk1) is a well known potent antagonist of this signaling pathway (31, 32). Previous studies show that Dkk1 has high affinity for LRP6 and inhibits Wnt/β-catenin signaling through binding to Kreman (Krm), a single-transmembrane protein (33, 34). The resultant Dkk1-LRP6-Krm complex removes LRP6 from the membrane via endocytosis, thereby attenuating Wnt/β-catenin signaling activation (35). The transmembrane and cytoplasmic domains of Krm are not required for triggering LRP6 endocytosis, suggesting that the functional endocytosis signal might reside within the LRP6 tail.

In the current study, we showed that the LRP6 mutant with defective tyrosine-based motifs exhibited increased cell surface distribution, a slower endocytosis rate, and a longer half-life when compared with wild-type LRP6. In addition, disruption of tyrosine-based motifs within the LRP6 tail increased its distribution on the lipid raft and its association with caveolin. Caveolin mediates clathrin-independent endocytosis through membrane invaginations on lipid raft forming caveolae (20). The uptake kinetics of caveolae-mediated endocytosis is much slower than that of clathrin-mediated endocytosis (36), which is the pathway necessary for LRP6 degradation (37). As a result, the altered distribution of LRP6 tyrosine mutant on the lipid raft is likely the cause of its slower endocytosis rate and a longer half-life. Mounting studies show that distinct internalization

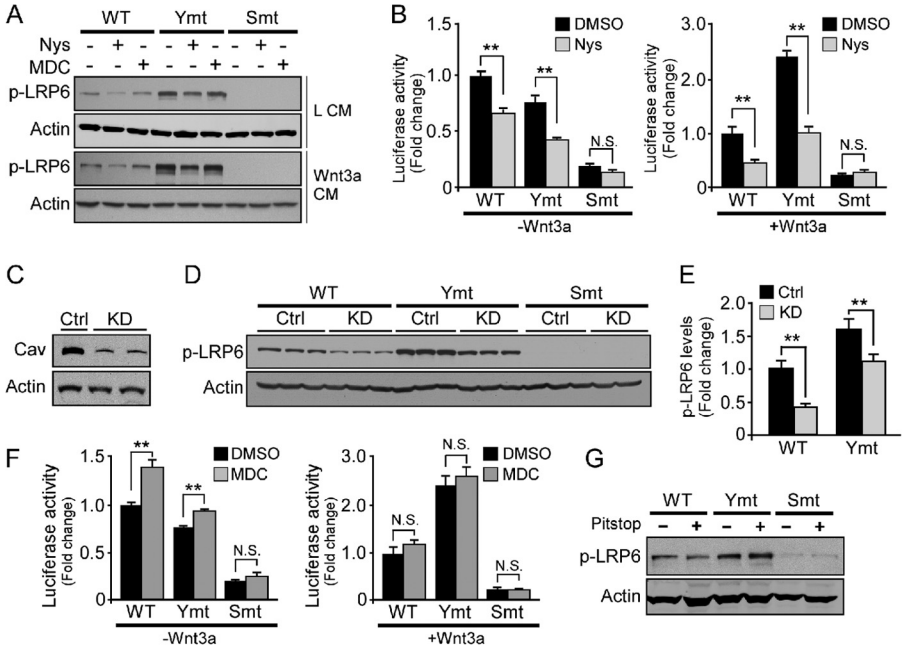

FIGURE 5. **Inhibition of caveolae-mediated endocytosis suppresses LRP6 phosphorylation and Wnt/β-catenin signaling activation.** *A*, cells expressing LRP6 WT or mutants were pretreated with or without Nys or MDC for 1 h prior to the addition of control CM or Wnt3a CM for an additional 2 h. LRP6 phosphorylation (*p-LRP6*) was examined by anti-phospho-LRP6 (Ser-1490) antibody. *Ymt*, tyrosine mutant; *Smt*, serine/threonine mutant. *B*, cells expressing WT or LRP6 mutants were pretreated with or without Nys for 1 h prior to incubation with control CM or Wnt3a CM for 2 h. Wnt/β-catenin signaling activity was evaluated with TOPFlash TCF-luciferase reporter assay. Data are representative of three independent experiments. Data represent mean ± S.D. *N.S.*, not significant; *, $p < 0.05$; **, $p < 0.01$. *DMSO*, dimethyl sulfoxide. *C*, cells were transfected with control or Cav-1-specific siRNA for 48 h, and the levels of Cav-1 and β-actin were examined by Western blot analysis. *Ctrl*, control; *KD*, knockdown. *D* and *E*, cells expressing LRP6 WT or mutants were transfected with control or Cav-1 siRNA for 48 h. LRP6 phosphorylation was examined by Western blot analysis (*D*) and quantified (*E*). *F*, cells expressing WT or LRP6 mutants were pretreated with or without MDC for 1 h prior to incubation with control CM or Wnt3a CM for 2 h. Wnt/β-catenin signaling activity was evaluated with TOPFlash TCF-luciferase reporter assay. *G*, cells expressing LRP6 WT or mutants were treated with 25 μM Pitstop 2, a selective clathrin inhibitor, for 15 min at 37 °C, and the level of LRP6 phosphorylation was examined by Western blot analysis.

routes and molecular machineries are utilized for either receptor degradation or signaling. The clathrin-mediated pathway plays a crucial role in terminating cell signaling by down-regulating transmembrane signaling receptors. For example, activated growth factor-induced epidermal growth factor receptors (EGFRs) are internalized and transported via endosomes to lysosomes for degradation in the presence of low level EGF, thus preventing the overgrowth of the cell (14, 15). On the other hand, epidermal growth factor receptors have been shown to be degraded in the lipid raft route and to be signaling in the clathrin-mediated route when the EGF level is high (16, 17). In the case of TGF-β signaling, both pathways play a role (18) depending on its adaptor protein Sara or Rap2. In these cases, the clathrin pathway is thought to direct receptors to a recycling pathway, thus protecting the receptors from degradation and supporting sustained signaling. Our results clearly showed that the LRP6 receptor utilizes an alternative mechanism in which the caveolae-dependent pathway promotes Wnt/β-catenin signaling transduction and the clathrin route mediates its degradation. Although it is unclear whether translocation of LRP6 to the lipid raft is a passive event, the disruption of tyrosine-based motifs in the LRP6 cytoplasmic tail may enhance its self-aggregation or association with lipid raft-resident proteins.

We also found that LRP6 levels were increased in the lipid raft microdomain after Wnt3a stimulation. Wnt3a treatment has been suggested to induce LRP6 aggregation at the plasma membrane, and the clustering of LRP6 provides a high local receptor concentration that may trigger LRP6 phosphorylation by CK1γ (9). It is possible that Wnt3a induces LRP6 oligomerization, which increases its affinity to lipid rafts where LRP6 can be phosphorylated and activated. Consistent with this notion, Fz5, which cooperates with LRP6 to activate the Wnt/β-catenin pathway, is internalized in a clathrin-dependent manner when it is expressed without LRP6 and Wnt, whereas the Wnt3a-Fz5-LRP6 complex is internalized through the caveolin-mediated pathway in response to Wnt3a (38). Interestingly, the LRP6 tyrosine mutant exhibited stronger phosphorylation and signaling activation in response to Wnt3a ligands, and these effects were suppressed by the caveolae inhibitor, nystatin. These findings indicate that the caveolae serve as a site for initiating ligand-induced LRP6 internalization. Acting as a signaling platform, this dynamic regulation could facilitate the integration of signaling molecules, thus ensuring specificity and efficiency in the signal transduction processes (39).

There are conflicting data on the internalization pathways of LRP6 and their roles in the activation of Wnt/β-catenin signaling. One study showed that Wnt3a induces the internalization of LRP6 through the clathrin-mediated pathway, leading to the accumulation of β-catenin (40). In contrast, another study suggested that internalization of LRP6 through caveolin, rather than clathrin, is necessary for the Wnt3a-dependent accumulation of β-catenin (38). Furthermore, it has been shown that Wnt3a promotes caveolae-mediated internalization of LRP6, whereas Dkk1 induces the internalization of LRP6 in a clathrin-dependent manner (37). A recent finding showed that the endocytic adaptor disabled-2 (Dab2), which inhibits Wnt/β-

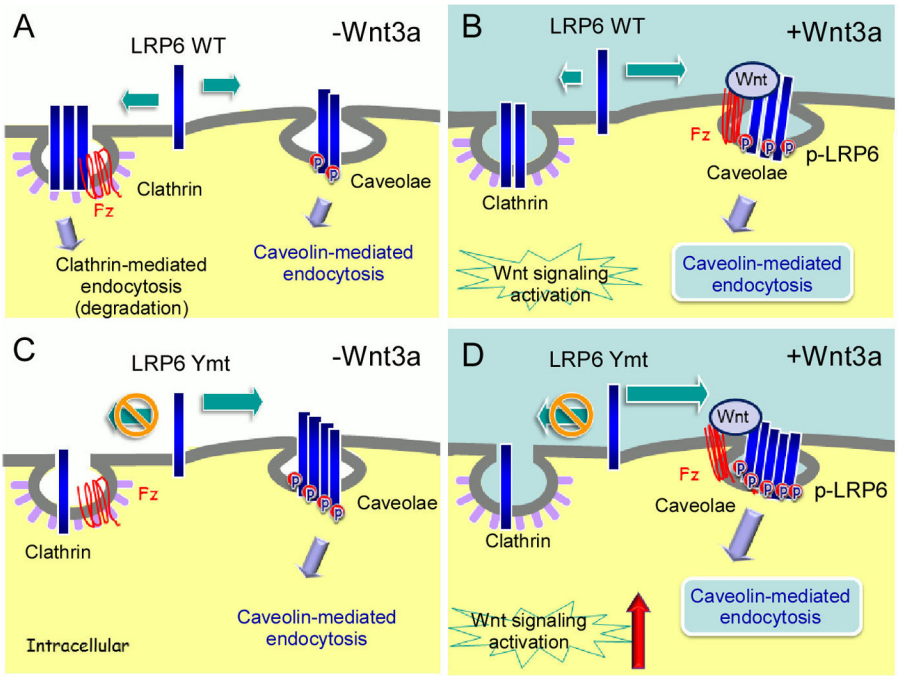

FIGURE 6. **Possible mechanism of LRP6 endocytosis and phosphorylation and their relationship to Wnt/β-catenin signaling activation.** *A*, in the absence of Wnt ligands, LRP6 is partitioned between lipid raft and non-lipid raft domains at the plasma membrane, which maintains basal levels of Wnt/β-catenin signaling. *B*, the binding of Wnts to LRP6 and Fz co-receptors promotes their translocation to lipid rafts, where LRP6 is accumulated, phosphorylated (*p-LRP6*), and internalized in a caveolin-dependent manner, which enhances Wnt/β-catenin signaling. *C* and *D*, when clathrin-mediated endocytosis of LRP6 is blocked due to defective endocytosis motifs, LRP6 is distributed mostly in the lipid raft domains. This increase of lipid raft partition of LRP6 leads to further enhanced phosphorylation of the receptor and Wnt/β-catenin signaling activation. *Ymt*, tyrosine mutant.

catenin signaling, shunts LRP6 toward the clathrin-dependent endocytic route (41). Although further experiments are necessary to confirm the relationship among Wnt/β-catenin signaling and the LRP6 endocytosis pathway, these events are likely regulated by the amount and subtype of Wnt ligands and/or the presence of adapter molecules.

Previous studies addressing the relationship between LRP6 endocytosis and signaling by exclusively using pharmacological inhibitors and siRNA approaches likely have potential caveats. These approaches perturb the entire clathrin or caveolae pathway, which could lead to nonspecific and/or indirect effects. It is possible that irrelevant receptors or pathways that rely on these internalization mechanisms might be altered, affecting LRP6 endocytosis and trafficking. Using LRP6 endocytosis mutants, herein we investigated the mechanism underlying LRP6 endocytosis, trafficking, and signaling without disturbing the endocytic pathways.

In summary, we demonstrate that tyrosine-based motifs within the LRP6 tail serve as an endocytosis signal that determines LRP6 internalization routes (Fig. 6). LRP6 is internalized by a mechanism involving both the clathrin-mediated and the caveolin-mediated pathways. Because Wnt ligands are associated with lipid raft due to their palmitoylation modification (42), the bindings of Wnts to LRP6 and Fz co-receptors promote their translocation to lipid rafts, where LRP6 might be more likely to accumulate and form "signalosomes" (9). Aggregated LRP6 is phosphorylated in this specialized microdomain and internalized in a caveolin-dependent manner, which activates Wnt/β-catenin signaling. When clathrin-mediated endocytosis of LRP6 is blocked due to defective endocytosis motifs, more LRP6 is distributed to the lipid rafts. The increase of lipid raft partition of LRP6 leads to an enhanced phosphorylation of the receptor and Wnt/β-catenin signaling activation in the tyrosine mutant. Our results shed light on the molecular mechanisms underlying LRP6 endocytosis and signaling and how the dynamic distribution of LRP6 between the clathrin and caveolin pathways plays a crucial role in regulating Wnt/β-catenin signaling. Taken together, understanding the dynamic regulation and pathological roles of LRP6 in Wnt signaling may help with developing therapeutic methods targeting this pathway.

Acknowledgments—We thank Henrietta Nielsen for discussion and the statistical analysis. We also thank Caroline Stetler for careful reading of this manuscript.

REFERENCES

1. Logan, C. Y., and Nusse, R. (2004) The Wnt signaling pathway in development and disease. *Annu. Rev. Cell Dev. Biol.* **20,** 781–810
2. Clevers, H. (2006) Wnt/β-catenin signaling in development and disease. *Cell* **127,** 469–480
3. Giles, R. H., van Es, J. H., and Clevers, H. (2003) Caught up in a Wnt storm: Wnt signaling in cancer. *Biochim. Biophys. Acta* **1653,** 1–24
4. Anastas, J. N., and Moon, R. T. (2013) WNT signalling pathways as therapeutic targets in cancer. *Nat. Rev. Cancer* **13,** 11–26
5. Boonen, R. A., van Tijn, P., and Zivkovic, D. (2009) Wnt signaling in Alzheimer's disease: up or down, that is the question. *Ageing Res. Rev.* **8,** 71–82
6. Papkoff, J., Brown, A. M., and Varmus, H. E. (1987) The *int*-1 proto-oncogene products are glycoproteins that appear to enter the secretory pathway. *Mol. Cell Biol.* **7,** 3978–3984
7. Wang, H. Y., Liu, T., and Malbon, C. C. (2006) Structure-function analysis of Frizzleds. *Cell. Signal.* **18,** 934–941

8. Brown, S. D., Twells, R. C., Hey, P. J., Cox, R. D., Levy, E. R., Soderman, A. R., Metzker, M. L., Caskey, C. T., Todd, J. A., and Hess, J. F. (1998) Isolation and characterization of *LRP6*, a novel member of the low density lipoprotein receptor gene family. *Biochem. Biophys. Res. Commun.* **248,** 879–888
9. Bilic, J., Huang, Y. L., Davidson, G., Zimmermann, T., Cruciat, C. M., Bienz, M., and Niehrs, C. (2007) Wnt induces LRP6 signalosomes and promotes Dishevelled-dependent LRP6 phosphorylation. *Science* **316,** 1619–1622
10. Tamai, K., Zeng, X., Liu, C., Zhang, X., Harada, Y., Chang, Z., and He, X. (2004) A mechanism for Wnt coreceptor activation. *Mol. Cell* **13,** 149–156
11. He, X., Semenov, M., Tamai, K., and Zeng, X. (2004) LDL receptor-related proteins 5 and 6 in Wnt/β-catenin signaling: arrows point the way. *Development* **131,** 1663–1677
12. Conner, S. D., and Schmid, S. L. (2003) Regulated portals of entry into the cell. *Nature* **422,** 37–44
13. Sorkin, A., and Von Zastrow, M. (2002) Signal transduction and endocytosis: close encounters of many kinds. *Nat. Rev. Mol. Cell Biol.* **3,** 600–614
14. Hanover, J. A., Willingham, M. C., and Pastan, I. (1984) Kinetics of transit of transferrin and epidermal growth factor through clathrin-coated membranes. *Cell* **39,** 283–293
15. Beguinot, L., Lyall, R. M., Willingham, M. C., and Pastan, I. (1984) Down-regulation of the epidermal growth factor receptor in KB cells is due to receptor internalization and subsequent degradation in lysosomes. *Proc. Natl. Acad. Sci. U.S.A.* **81,** 2384–2388
16. Choi, S. C., Kim, G. H., Lee, S. J., Park, E., Yeo, C. Y., and Han, J. K. (2008) Regulation of activin/nodal signaling by Rap2-directed receptor trafficking. *Dev. Cell* **15,** 49–61
17. Sigismund, S., Argenzio, E., Tosoni, D., Cavallaro, E., Polo, S., and Di Fiore, P. P. (2008) Clathrin-mediated internalization is essential for sustained EGFR signaling but dispensable for degradation. *Dev. Cell* **15,** 209–219
18. Di Guglielmo, G. M., Le Roy, C., Goodfellow, A. F., and Wrana, J. L. (2003) Distinct endocytic pathways regulate TGF-β receptor signalling and turnover. *Nat. Cell Biol.* **5,** 410–421
19. Gong, Q., Huntsman, C., and Ma, D. (2008) Clathrin-independent internalization and recycling. *J. Cell Mol. Med.* **12,** 126–144
20. Parton, R. G., Hanzal-Bayer, M., and Hancock, J. F. (2006) Biogenesis of caveolae: a structural model for caveolin-induced domain formation. *J. Cell Sci.* **119,** 787–796
21. Le Roy, C., and Wrana, J. L. (2005) Clathrin- and non-clathrin-mediated endocytic regulation of cell signalling. *Nat. Rev. Mol. Cell Biol.* **6,** 112–126
22. Razani, B., Woodman, S. E., and Lisanti, M. P. (2002) Caveolae: from cell biology to animal physiology. *Pharmacol. Rev.* **54,** 431–467
23. Chen, W. J., Goldstein, J. L., and Brown, M. S. (1990) NPXY, a sequence often found in cytoplasmic tails, is required for coated pit-mediated internalization of the low density lipoprotein receptor. *J. Biol. Chem.* **265,** 3116–3123
24. Trowbridge, I. S., Collawn, J. F., and Hopkins, C. R. (1993) Signal-dependent membrane protein trafficking in the endocytic pathway. *Annu. Rev. Cell Biol.* **9,** 129–161
25. Lefkowitz, R. J. (1998) G protein-coupled receptors. III. New roles for receptor kinases and β-arrestins in receptor signaling and desensitization. *J. Biol. Chem.* **273,** 18677–18680
26. Li, Y., Marzolo, M. P., van Kerkhof, P., Strous, G. J., and Bu, G. (2000) The Y*XX*L motif, but not the two NP*X*Y motifs, serves as the dominant endocytosis signal for low density lipoprotein receptor-related protein. *J. Biol. Chem.* **275,** 17187–17194
27. Liu, C. C., Prior, J., Piwnica-Worms, D., and Bu, G. (2010) LRP6 overexpression defines a class of breast cancer subtype and is a target for therapy. *Proc. Natl. Acad. Sci. U.S.A.* **107,** 5136–5141
28. Hsieh, J. C., Lee, L., Zhang, L., Wefer, S., Brown, K., DeRossi, C., Wines, M. E., Rosenquist, T., and Holdener, B. C. (2003) Mesd encodes an LRP5/6 chaperone essential for specification of mouse embryonic polarity. *Cell* **112,** 355–367
29. Li, Y., Chen, J., Lu, W., McCormick, L. M., Wang, J., and Bu, G. (2005) Mesd binds to mature LDL-receptor-related protein-6 and antagonizes ligand binding. *J. Cell Sci.* **118,** 5305–5314
30. Clevers, H., and Nusse, R. (2012) Wnt/β-catenin signaling and disease. *Cell* **149,** 1192–1205
31. Niehrs, C. (2006) Function and biological roles of the Dickkopf family of Wnt modulators. *Oncogene* **25,** 7469–7481
32. Bafico, A., Liu, G., Yaniv, A., Gazit, A., and Aaronson, S. A. (2001) Novel mechanism of Wnt signalling inhibition mediated by Dickkopf-1 interaction with LRP6/Arrow. *Nat. Cell Biol.* **3,** 683–686
33. Bafico, A., Gazit, A., Pramila, T., Finch, P. W., Yaniv, A., and Aaronson, S. A. (1999) Interaction of frizzled related protein (FRP) with Wnt ligands and the frizzled receptor suggests alternative mechanisms for FRP inhibition of Wnt signaling. *J. Biol. Chem.* **274,** 16180–16187
34. Semënov, M. V., Tamai, K., Brott, B. K., Kühl, M., Sokol, S., and He, X. (2001) Head inducer Dickkopf-1 is a ligand for Wnt coreceptor LRP6. *Curr. Biol.* **11,** 951–961
35. Mao, B., Wu, W., Davidson, G., Marhold, J., Li, M., Mechler, B. M., Delius, H., Hoppe, D., Stannek, P., Walter, C., Glinka, A., and Niehrs, C. (2002) Kremen proteins are Dickkopf receptors that regulate Wnt/β-catenin signalling. *Nature* **417,** 664–667
36. Beer, C., Andersen, D. S., Rojek, A., and Pedersen, L. (2005) Caveola-dependent endocytic entry of amphotropic murine leukemia virus. *J. Virol.* **79,** 10776–10787
37. Yamamoto, H., Sakane, H., Yamamoto, H., Michiue, T., and Kikuchi, A. (2008) Wnt3a and Dkk1 regulate distinct internalization pathways of LRP6 to tune the activation of β-catenin signaling. *Dev. Cell* **15,** 37–48
38. Yamamoto, H., Komekado, H., and Kikuchi, A. (2006) Caveolin is necessary for Wnt-3a-dependent internalization of LRP6 and accumulation of β-catenin. *Dev. Cell* **11,** 213–223
39. Simons, K., and Toomre, D. (2000) Lipid rafts and signal transduction. *Nat. Rev. Mol. Cell Biol.* **1,** 31–39
40. Blitzer, J. T., and Nusse, R. (2006) A critical role for endocytosis in Wnt signaling. *BMC Cell Biol.* **7,** 28
41. Jiang, Y., He, X., and Howe, P. H. (2012) Disabled-2 (Dab2) inhibits Wnt/β-catenin signalling by binding LRP6 and promoting its internalization through clathrin. *EMBO J.* **31,** 2336–2349
42. Komekado, H., Yamamoto, H., Chiba, T., and Kikuchi, A. (2007) Glycosylation and palmitoylation of Wnt-3a are coupled to produce an active form of Wnt-3a. *Genes Cells* **12,** 521–534